Metastability Studies of Syndiotactic Polystyrene Polymorphism

Rong-Ming Ho,*,† Chien-Pang Lin,† Hsien-Yin Tsai,‡ and Ea-Mor Woo§

Department of Chemical Engineering, National Chung Hsing University, Taichung 40227, Taiwan, R.O.C.; Union Chemical Laboratories, Industrial Technology Research Institute, Hsinchu 30055, Taiwan, R.O.C.; and Department of Chemical Engineering, National Cheng Kung University, Tainan, 70101, Taiwan, R.O.C.

Received April 18, 2000; Revised Manuscript Received June 21, 2000

ABSTRACT: Polymorphic behavior (i.e., the development of α and β forms) of melt-crystallized syndiotactic polystyrene, sPS, has been studied by structure analysis of FTIR (Fourier transform infrared spectroscopy), WAXD (wide-angle X-ray diffraction), and ED (electron diffraction) as well as thermal analysis of DSC (differential scanning calorimetry). Significant factors that influence the formation of polymorphism were examined and described. Isolated α crystals and β crystals of sPS crystallized at different crystallization temperatures from the melt have been obtained. The equilibrium melting temperatures, T_m^o, of both forms were determined by using linear Hoffman−Weeks (H−W) extrapolation and nonlinear H−W treatment. The T_m^o (i.e., structural metastability) of β form in sPS was found to be higher than that of α form. The occurrence of phase stability inversion with lamellar size (i.e., morphological metastability) in sPS was recognized. Transformations from α to β phase in the stage of crystal growth or in the heating scanning process have been evidenced. The interlinkage of structural metastability and morphological metastability in sPS polymorphism was examined. The behavior of phase transformation has been successfully interpreted in terms of the stability inversion phase diagram. The formation of the α form is indeed a kinetic result of crystallization.

Introduction

Polymorphism of syndiotactic polystyrene (sPS) has been extensively studied in recent years. Structural studies by using X-ray diffraction,[1−8] electron diffraction,[8−14] Fourior transform infrared radiation,[15−23] and solid-state NMR[24−27] have shown a very complex polymorphic behavior for this polymer. Two types of melt-crystallized crystal structures have been identified and described in terms of α and β, both containing the planar-zigzag conformation of backbone chains. The crystalline β form is characterized by orthorhombic chain packing, whereas the crystalline α form is characterized by trigonal chain packing. These melt-crystallized crystalline forms are further complicated by different degrees of structural order. They are two limited disordered modifications, α′ and β', and two limited ordered modifications, α″ and β''. Two types of solvent-induced crystal structures have also been found. They are γ and δ, both containing the helical conformation of backbone chains.

Many studies have been devoted to understanding the crystallization effects on polymorphic behavior, and complex behavior has been found.[1−4,16,23] The formation of the α form is, in general, believed to be either the result of kinetically controlled process or the memory effect of α nuclei. The formation of thermally crystallized polymorphism (i.e., α and β forms) is dependent upon thermal histories and crystallization conditions such as annealing temperature, cooling rate to crystallization temperature, crystallization temperature, and so on. Studies on sPS have been carried out in order to correlate multiple melting with polymorphism.[28−34] The complexity of lamellar reorganization with polymorphic transformation gives rise to arguments with the assignment of different crystal types to the multiple melting. The behavior of phase transformation between α and β forms becomes a controversial issue.

Recently, the role of metastability in polymer phase transitions has been thoroughly discussed and examined by Keller and Cheng.[35] In addition to classical metastability that describes the phase transformation from one state to another according to the Ostwald stage rule,[36] circumstantial metastability, including morphological, compositional, and other types of metastability, was proposed and believed to be essentially important while the behavior of phase transitions of polymers is discussed. The circumstantial metastability represents any state that has failed to attain its ultimate stability and may be arrested at one of multiple local minima in the Gibbs free energy profile due to kinetic restrictions of the phase transformation. The morphological metastability of this restricted state is associated with phase size (i.e., lamellar thickness) and can be experimentally observed in the course of a slow transformation when compared on the time scale of our observations. According to this conceptual description of metastability, the metastability of melt-crystallized sPS polymorphism shall include the classical metastability concerning structural essence and the morphological metastability concerning lamellar size. As is well-known, polymeric crystals are lamellae containing chains in a folded conformation with the lamellar thickness equal or related to the fold length.[37] In an isothermal crystallization process, the lamellar thickness is determined by the prevailing undercooling, ΔT.[38] The morphological metastability is, thus, varied with crystallization temperature. The behavior of polymorphic transformation may change with the crystallization temperature since the dependence of the lamellar thickness on ΔT in α crystal form may be different from the β crystal form.

* To whom all correspondence should be addressed. Tel 886-4-2857471; Fax 886-4-2854734; e-mail rmho@dragon.nchu.edu.tw.
† National Chung Hsing University.
‡ Industrial Technology Research Institute.
§ National Cheng Kung University.

10.1021/ma000666d CCC: $19.00
Published on Web 08/05/2000

In other words, the metastability of polymorphism may invert with lamellar size where a stable phase defined by the structural metastability can become a metastable phase due to the influence of phase dimensions. This behavior is described as a phenomenon of stability inversion with crystal size.[35,39]

In this study, we attempted to explore the metastability of sPS polymorphism by first determining the equilibrium melting temperature, T_m^o. The T_m^o of crystalline polymers is defined as the melting temperature of an infinite stack of extended chain crystals so that the structural metastability of polymorphism can be measured. According to the determined values of T_m^o in α and β crystals, the behavior of phase transformation in melt-crystallized sPS was then examined by experimental characterization. The formation of metastable α crystals as well as the transformation from α to β crystals can be well described in terms of the behavior of phase stability inversion. The studies on the metastability of sPS polymorphism provide an excellent paragon to explore the effects of classical metastability and circumstantial metastability in polymer phase transitions.

Experimental Section

Materials. Semicrystalline syndiotactic polystyrene was obtained as courtesy sample materials from Union Chemical Laboratories. The number-average molecular weight of the samples is 67 000 g/mol, and the polydispersity is 3.5.

Differential Scanning Calorimetry (DSC). DSC experiments were carried out in a Perkin-Elmer DSC 7. The temperature and heat flow scales at different heating rates were carefully calibrated using standard materials. The samples were first heated to the maximum annealing temperature, T_{max}, for 5 min in order to eliminate the crystalline residues formed during the preparation procedure of sPS. The T_{max} is also known as residential temperature.[40] The polymer samples were then cooled at a rate of 150 °C/min to a preset temperature, T_c, for isothermal crystallization. The crystallization time, t_c, was about 10 times of exothermic peak time, t_p, to completing crystallization. The value of t_p was determined by the exothermic process of isothermal crystallization. To study the transformation behavior, the isothermal crystallization was carried out at different isothermal times. The consecutive heating was performed at different heating rates ranging from 10 to 40 °C/min. The DSC sample size was around 5 mg for all the melting behavior studies. Each measurement was performed at least twice. Thermal degradation after high-temperature treatment may lead to significant changes in melting behavior. To alleviate the problem, the testing sample having high annealing temperature (i.e., T_{max} is 345 °C) was used only once each time for DSC measurements. No evidence of severe degradation problem was found in DSC analysis.

Wide-Angle X-ray Diffraction (WAXD). For WAXD experiments, the same crystallization conditions as described in previous section were carried out on sPS bulk samples. A Siemens D5000 1.2 kW tube X-ray generator (Cu Kα radiation) with a diffractometer was used for WAXD powder experiments. The scanning 2θ angle ranged between 5° and 40° with a step scanning of 0.05° for 3 s. The diffraction peak positions and widths observed from WAXD experiments were carefully calibrated with silicon crystals with known crystal size.

Fourier Transform Infrared Spectroscopy (FTIR). The sPS powders were hot-pressed to form thin films. The thin film samples were then thermally treated in an Instec STC200 hot stage for different crystallization conditions as previously described. Infrared spectra were obtained via Perkin-Elmer Paragon 500 FTIR at a resolution 1.0 cm^{-1}. The frequency scale was internally calibrated using a He−Ne laser, and 30−300 scans were signal-averaged to reduce the noise. The scanned wavenumber range was 4000−450 cm^{-1}.

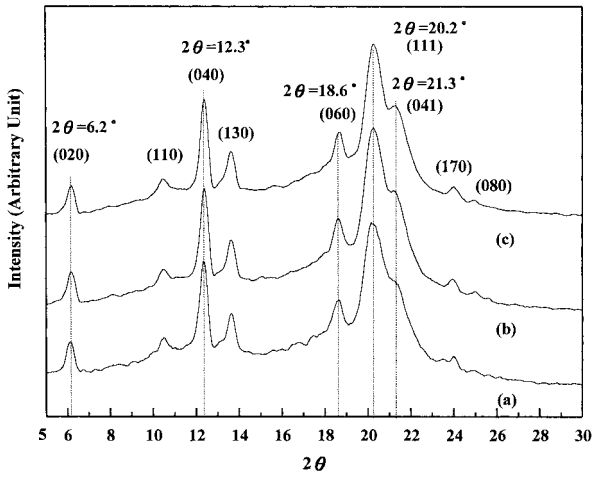

Figure 1. WAXD diffraction patterns of sPS crystallized at (a) $T_c = 240$, (b) 245, and (c) 250 °C for $t_c = 10t_p$ from the melt ($T_{max} = 345$ °C).

Electron Diffraction (ED). The sPS ultrathin films with thickness in the range of 10 nm for ED experiments were prepared by casting a 0.2% (w/w) sPS and xylene solution onto carbon-coated glass slides. The sPS samples were then crystallized at different crystallization temperatures from the melt. The thermal treatments were similar to the samples for DSC measurements. After crystallization, the films were quenched into ice water. The quenched samples were shadowed by Pt and coated with carbon again. After shadowing, the sPS films were stripped and floated onto the water surface and then recovered using copper grids. The ED patterns of sPS were obtained via a JEOL (JEM-1200×) TEM using an accelerating voltage of 120 kV. Calibration of the electron diffraction spacing was carried out using Au and TlCl (d-spacing < 3.84 Å, the largest spacing for TlCl). Spacing values larger than 3.84 Å were calibrated by doubling the d-spacings of these reflections.

Results and Discussion

Formation of Polymorphism. The complex polymorphic behavior of sPS was systematically studied by analyzing a series of isothermally melt-crystallized sPS samples. These melt-crystallized samples were thoroughly examined using WAXD and FTIR to identify their corresponding crystal structures (i.e., single α form, single β form, or mixed forms). Figure 1 shows the WAXD powder patterns of sPS crystallized at various temperatures from the melt of $T_{max} = 345$ °C. Figure 2 shows the corresponding FTIR spectra. As shown, the characteristic diffraction peaks of β' form (i.e., $2\theta \cong 6.2^o$, 12.3^o, 18.6^o, 20.2^o, and 21.3^o) in WAXD patterns and the characteristic absorption of β' form (i.e., absorption at around 858 and 911 cm^{-1}) in FTIR spectra were clearly observed in all three samples. The absorption at around 905 and 840 cm^{-1} is attributed to the amorphous portions of sPS. Similar results were found in other samples crystallized at different temperatures. In other words, only single β' phase was formed in these samples. In contrast to high annealing temperature, low-T_{max} samples (T_{max} is below 300 °C) only exhibit the entity of the α″ form as shown in Figure 3 (characteristic peaks at $2\theta \cong 6.7^o$, 11.7^o, 14.0^o, 20.3^o, and 15.6^o) for WAXD results and in Figure 4 (the characteristic absorption at around 851 and 901 cm^{-1}) for FTIR results. The absorption at around 840 cm^{-1} is also attributed to the amorphous portions of sPS. These results suggest that isolated α″ crystals and β' crystals can be obtained by simply adjusting the annealing temperature.

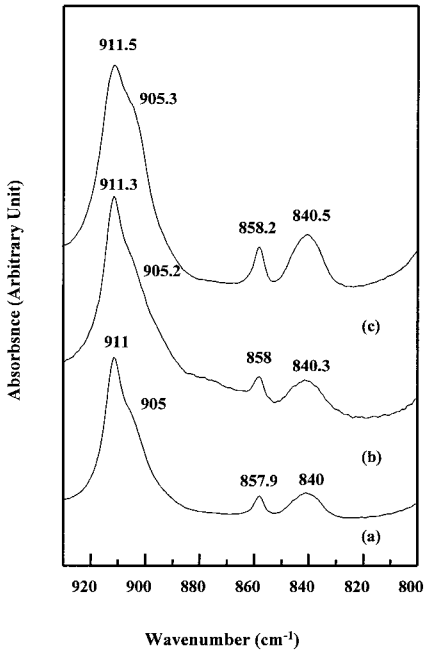

Figure 2. FTIR spectra of sPS crystallized at (a) $T_c = 240$, (b) 245, and (c) 250 °C for $t_c = 10t_p$ from the melt ($T_{max} = 345$ °C).

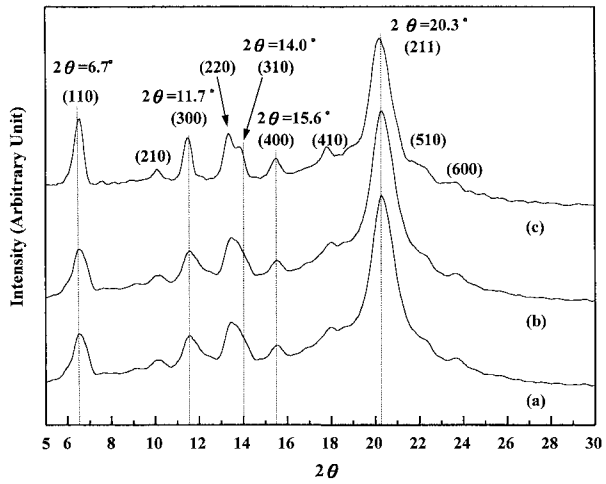

Figure 3. WAXD diffraction patterns of sPS crystallized at (a) $T_c = 235$, (b) 240, and (c) 245 °C for $t_c = 10t_p$ from the melt ($T_{max} = 290$ °C).

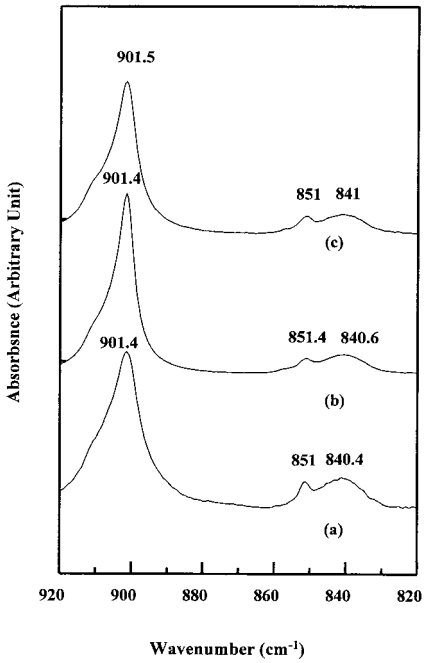

Figure 4. FTIR spectra of sPS crystallized at (a) $T_c = 235$, (b) 240, and (c) 245 °C for $t_c = 10t_p$ from the melt ($T_{max} = 290$ °C).

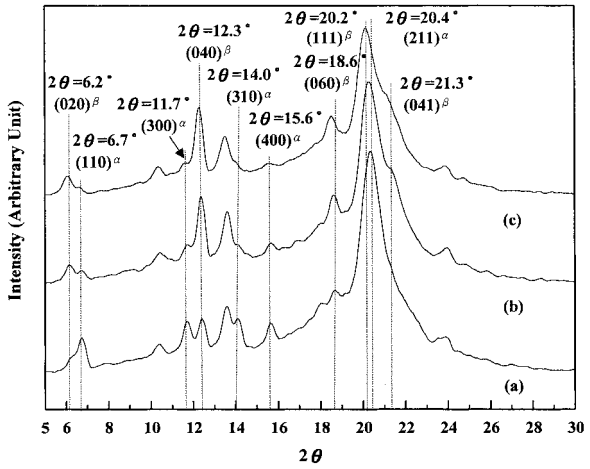

Figure 5. WAXD diffraction patterns of sPS crystallized at (a) $T_c = 235$, (b) 240, and (c) 245 °C for $t_c = t_p$ from the melt ($T_{max} = 300$ °C).

Isothermal crystallization of sPS is usually carried out from the melt after annealing at the T_{max} ranging from 300 to 340 °C. These melt-crystallized samples generally contain mixed α and β phases. Different speculations and suggestions have been proposed to correlate the polymorphic behavior to the multiple melting behavior of DSC heating traces, but there is still a great deal of arguments about this correlation. This study was also in the same dilemma. The proportion of α phase to β phase was varied from one examined sample to another. These crystallized samples all involved complicated melting behaviors with multiple endothermic peaks even for samples crystallized with single β phase. The assignment of endothermic peaks corresponding to melting of crystal phases is difficult to rationalize. We found that the pretreatment of sPS raw materials was very critical to the reproducibility of experimental results. In this study, the raw materials of sPS pellets was dissolved into xylene at 135 °C for 4 h and then discharged into methanol for precipitation. We have found that the problem of reproducibility may alleviate after the treatment of precipitation. We speculate that the improvement is attributed to the achievement of well-controlled thermal history for sPS raw materials before crystallization. Figure 5 shows the WAXD results of sPS crystallized at different temperatures from the melt of $T_{max} = 300$ °C. The proportion of β' phase to α'' phase, approximately determined from the relative intensity of diffraction peak at $2\theta \sim 12.3°$ of β' form to diffraction peak at $2\theta \sim 11.7°$ of α'' form, has been found to dramatically change with crystallization temperature. The lower the crystallization temperature, the greater the fraction of α crystals. At high enough T_c, only the β phase was observed. It was also interesting to discover that the formation of mixed forms is dependent upon the crystallization time. The shorter the crystallization time, the larger the fraction of α crystals. When the crystallization time is long enough, there is only β form crystals left as illustrated in Figure 6b. However, the effect of crystallization time on the population of mixed

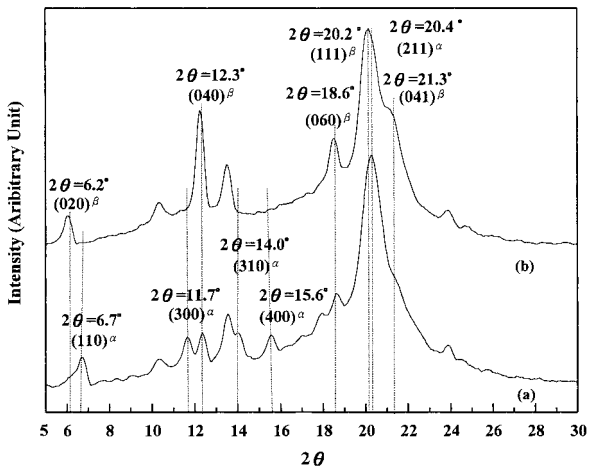

Figure 6. WAXD diffraction patterns of sPS crystallized at T_c = 237.5 °C for (a) $t_c = t_p$ and (b) $t_c = 10t_p$ from the melt (T_{max} = 300 °C).

forms becomes insignificant while the T_{max} is above 340 °C. According to the experimental results, significant factors that influence the formation of polymorphism were found to be maximum annealing temperature (T_{max}), crystallization temperature (T_c), and crystallization time (t_c). It was also noted that the T_{max} for melt crystallization seems the primary factor to determine the formed structure. The probability for formation of α crystals raises become greater for samples treated at lower T_{max}. At high T_{max} temperature (above 340 °C), the occurrence of α form in the melt-crystallized samples becomes trivial.

Certainly, the effect of annealing time at T_{max} also influences the formation of polymorphism. It has been reported by Guerra and co-workers that crystals with single β form can be obtained for melt-crystallized samples after long annealing time (say a hour) at T_{max} = 300 °C.[1] For the sake of simplicity, the suggested guide for the formation of polymorphism was based on the results of short annealing time (i.e., 5 min) for all of the experiments since this time scale is more reasonable for crystallization experiments. The cooling rate from the melt is another factor that is usually discussed in sPS polymorphic studies. It has been reported that the fraction of α crystals increases with the increasing of cooling rate. In this study, we have found that the effect of cooling rate is not so profound for the polymorphic behavior as long as crystallization temperature is not too close to or passes over the temperature of maximum crystallization rate.

As a result, the formation of polymorphism is determined by first considering the maximum annealing temperature (T_{max}) and then the crystallization temperature (T_c) and crystallization time (t_c). Samples annealed at T_{max} = 345 °C only generate β crystals. While samples are annealed at T_{max} = 290 °C, crystals with single α form are obtained. There are no significant effects of crystallization temperature and time on the formation of polymorphism in both cases. Only if samples annealed at T_{max} between 300 and 340 °C may crystals with mixed phases form. The probability to form α crystals increases while the T_c and/or t_c decrease. The T_{max} effect on the formation of polymorphism leads to an essential question of whether or not the nucleation seeds decide their final crystalline structures.

Structural Metastability of Polymorphic sPS. To explore the possible explanations for the observed

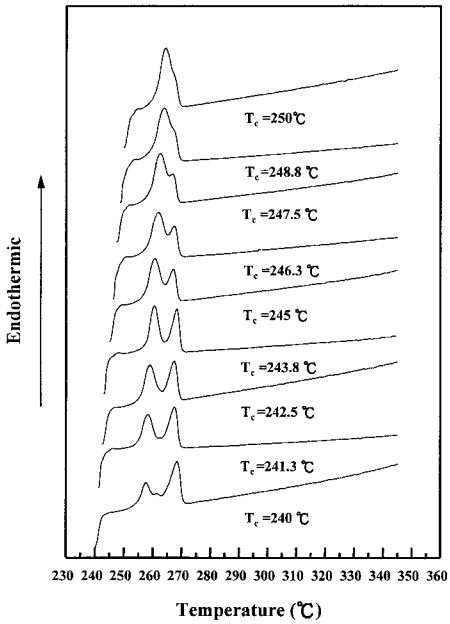

Figure 7. DSC thermograms of sPS crystallized at different T_c from the melt (T_{max} = 345 °C). The heating rate is 10 °C/min for all the scans.

results of polymorphic behavior, it is necessary to understand the differences in T_m^o of sPS polymorphism. According to the previous results of polymorphic analysis, corresponding melting behavior was studied by using differential scanning calorimetry. Figure 7 shows the melting traces of sPS crystallized at different temperatures from the melt of T_{max} = 345 °C. These are associated with the melting of β' crystals. The DSC traces exhibit multiple endothermic peaks. Two major endothermic peaks were found. The location of the high melting peak is almost independent of the crystallization temperature at the same heating rate. The corresponding enthalpies of the melting peaks show, however, a significant change with heating rate as shown in Figure 8. The melting enthalpy decreases with the increasing of heating rate, while the total enthalpy of the high melting and of the low melting is near constant at different heating rates. This result indicates that reorganization is carried out during heating. At a slow heating rate, the original crystals with the lower melting reorganize to reach a higher degree of perfection of lamellae and/or to become thicker lamellae (i.e., higher melting temperature crystals). The processes of perfection and thickening are strongly suppressed when heating is too rapid to accomplish the reorganization. To explore the process of the reorganization, melt-crystallized samples having reheating treatment were prepared for WAXD measurements. They show similar WAXD results having reflections of β' form after reheating process. We speculate that the reorganization mainly involves a lamellar thickening process since the perfection process of β' phase to β'' phase does not appear.

For the low melting peaks, a linear relationship between the observed melting peak temperatures (T_m) and the isothermal crystallization temperatures (T_c) was found. The Hoffman−Weeks extrapolation is, therefore, applied to obtain an extrapolated temperature according to

$$T_m = T_m^o(1 - 1/\gamma) + T_c/\gamma$$

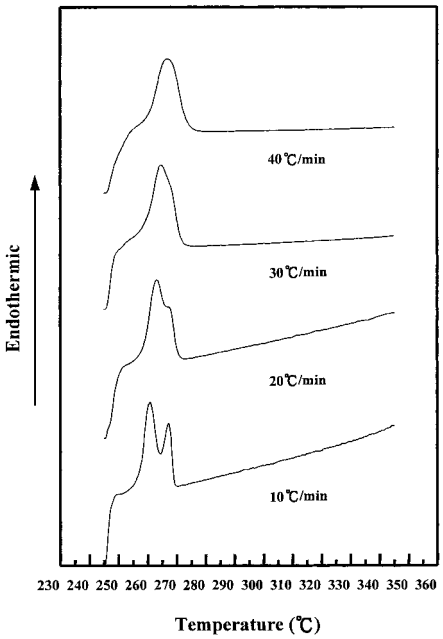

Figure 8. Heating rate effect on DSC thermograms of sPS crystallized at 245 °C from the melt (T_{max} = 345 °C).

where $T_m°$ is the equilibrium melting temperature, and $\gamma = l/l^*$ is the ratio of lamellar thickness l to the thickness l^* of the critical nucleus at T_c. Different methods including the Gibbs−Thomson approach,[41] the Hoffman−Weeks procedure,[42] and the growth rate data fitting[43] have been used to determine $T_m°$. Among them, the Hoffman−Weeks method has been commonly utilized and accepted for the determination of $T_m°$ due to its straightforward experimental implementation and its analytical simplicity. However, thermal lag of a DSC cell inevitably causes a shift of melting peak to a higher temperature, especially when a high thermal resistance sample such as a polymer material is studied.[44] A lower heating rate should be chosen for scanning in order to reduce the shift that may cause significant error in extrapolated value. It is common that reorganization or recrystallization processes are taking place during heating to obtain crystals with higher metastability. Multiple melting peaks are, thus, present. This may lead to difficulty in determining the true melting point when the multiple melting points appear very close to each other or a significant error (lower value) in melting point determination due to the overlapping of simultaneous endothermic and exothermic reactions.[45] Higher heating rates are needed to prevent reorganization or recrystallization. For these reasons, the peak maximum temperature should be determined by an optimum heating rate scanning, even though an error is always present with the best conditions. A possible way to eliminate the error has been reported by Illers et al.[42] According to the theory of heat-flow calorimeters, the increase in the observed maximum peak temperature is proportional to the square root of the heating rate, thermal resistance, heat of fusion, and sample mass. A corrected equation for the shift in the melting temperature was derived as follows:

$$\Delta T_m = T_{m,p} - T_{m,0} = (2W\Delta HRQ)^{1/2}$$

where $T_{m,p}$ is the observed maximum peak melting temperature at heating rate β, $T_{m,0}$ the true melting temperature without thermal lag effect, W the sample weight used for DSC measurement, ΔH the heat of fusion per gram of the sample used for DSC measurements, R the thermal resistance of the sample, and Q the heating rate of DSC measurement.

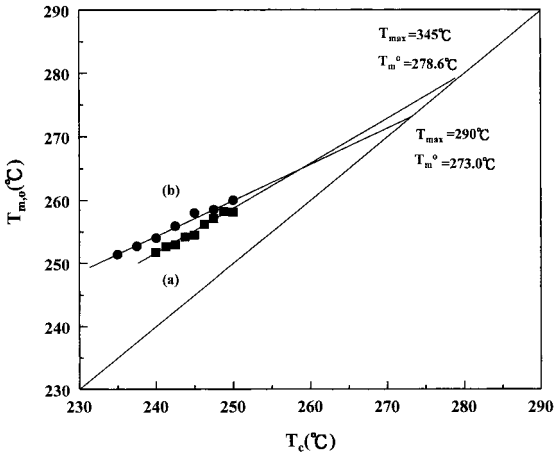

Figure 9. Hoffman−Weeks extrapolation for sPS crystallized from the melt (a) (T_{max} = 345 °C) and (b) (T_{max} = 290 °C) by using the corrected peak melting temperatures.

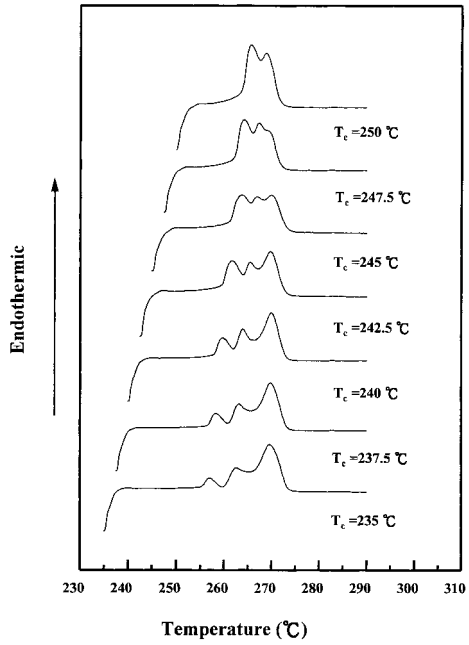

Figure 10. DSC thermograms of sPS crystallized at different T_c from the melt (T_{max} = 290 °C). The heating rate is 10 °C/min for all the scans.

By plotting the melting peak temperatures as a function of the square root of heating rate at constant sample weight and linearly extrapolating to zero heating rate, the true melting point ($T_{m,0}$) can be obtained. After the correction in temperature shift, the Hoffman−Weeks extrapolation is applied to obtain the extrapolated temperatures as shown in Figure 9a. The equilibrium melting temperature of β form is determined as 278.6 °C.

Similar methods were also carried out on the melting behavior of α form crystals. Figure 10 shows the melting traces of sPS crystallized at different temperatures from the melt of T_{max} = 290 °C. Complex melting behavior was found. The majority of these DSC heating traces exhibited three major endothermic peaks. The highest melting has been identified as the melting of reorganized lamellar crystals on the basis of experimental

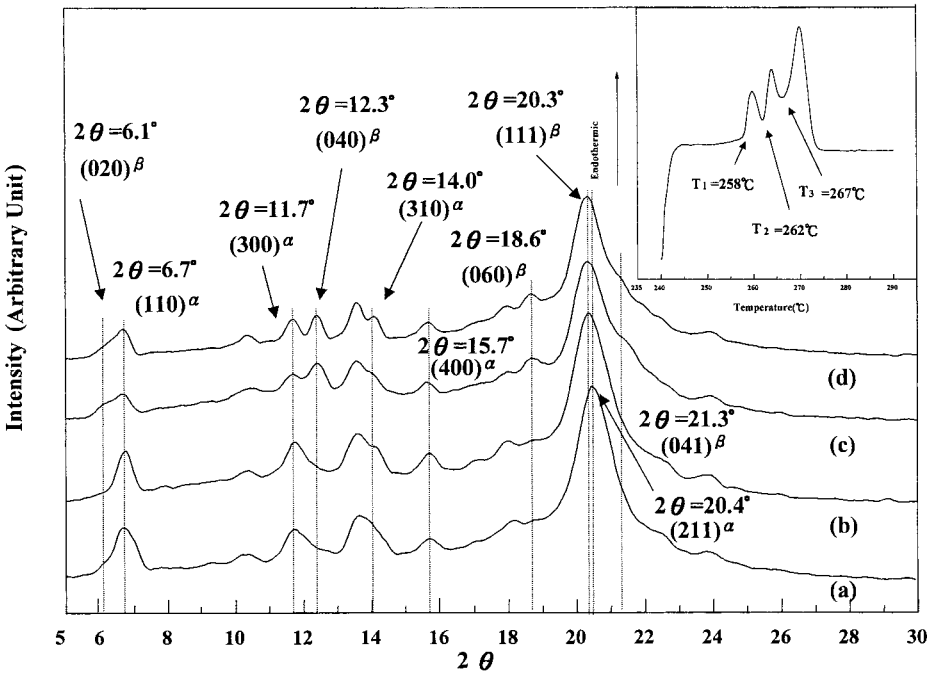

Figure 11. WAXD diffraction patterns for sPS crystallized at T_c = 240 °C from the melt (T_{max} = 290 °C): (a) before reheating, (b) after reheating to 258 °C, (c) after reheating to 262 °C, and (d) after reheating to 267 °C. Inner set shows a corresponding DSC thermogram (10 °C/min).

evidences similar to above. For the lowest melting, a linear relationship between the $T_{m,0}$ and the T_c was found. The Hoffman−Weeks extrapolation is applied to obtain the equilibrium temperatures as shown in Figure 9b. The equilibrium melting temperature of α form is determined as 273.1 °C.

The peak temperatures of intermediate melting have been found to increase with crystallization temperatures. To explore the origins of this intermediate melting, a series of melt-crystallized samples having specific reheating processes were prepared for WAXD measurements. The sPS samples were reheated at constant heating rate, the same rate as DSC heating measurements, to a specific temperature after isothermal crystallization. The reheated samples were then rapidly cooled to 30 °C and then examined by using WAXD. Their corresponding WAXD results reflect plausible discoveries as an illustration in Figure 11. Significant changes in WAXD reflections of α form have not been found while the reheating temperature was below the onset of lowest melting peak, 258 °C (see Figure 11a,b). However, the characteristic reflections of β phase started appearing while the reheating temperature reached the end of lowest melting, 262 °C (Figure 11c). Further heating the samples to the end of intermediate melting (267 °C) only brought slight change in the population of mixed forms (Figure 11d). These observations suggest that the lowest melting peak shall correspond to the melting of individual α form. Within the temperature range of lowest melting, the initial α crystals may either reorganize to thicker α crystals or transform to β crystals. The intermediate melting thus involves a lamellar thickening process and transformation of α to β phase combining with the possibility of β form reorganization (see next section for detailed explanations).

It is evident that the equilibrium melting temperature of β form is higher than that of α form. This result reflects that melt-crystallized samples at different T_{max} may possess various types of residual nuclei. As a result, the residual nuclei thus affect the consequential crystal structure after crystallization. At lower T_{max}, the probability to endure α nuclei certainly increases. It has been proposed that the T_{max} effect on the formation of polymorphism may be attributed to the memory effect of nucleus, and the formation of α crystals is governed by the nucleation seeds of α form.[1,2] However, this justification is not always true for our experimental results. For instance, samples crystallized at T_c = 240 °C from the melt of T_{max} = 345 °C was annealed at 290 °C and then crystallized at T_c = 240 °C again. Crystals with α form were obtained after this thermal treatment. This result indicates that there are possibilities to generate α crystals from β nuclei. As a result, we suggest that the formation of polymorphism in sPS shall be primarily determined by crystallization kinetics. At lower nucleation barrier, the crystallization tends to form α crystals. When the residual nuclei are completely annihilated, samples crystallized as β crystals from the melt due to high nucleation barrier (see next section for detailed interpretations).

More recently, the validity of the Hoffman−Weeks extrapolation for the determination of T_m^o of polymers has been critically reviewed by Marand et al.[46,47] Their results indicated that the linear extrapolation invariably underestimates the T_m^o. The disagreement starts from the treatment of the experimentally observed undercooling ($\Delta T = T_m^o - T_c$) dependence of the initial lamellar thickness, $l^* = C_1/\Delta T + C_2$. The C_1 and C_2 are constants, obtained experimentally. The value of C_2 is ignored in the classical Hoffman−Weeks treatment. It has been argued that the observed melting temperature must vary nonlinearly with the crystallization temperature while the term C_2 cannot be ignored. Therefore, a nonlinear Hoffman−Weeks extrapolation has been proposed for T_m^o determination.[47] By plotting $M = T_m^o/(T_m^o - T_m)$ versus $X = T_m^o/(T_m^o - T_c)$ for different choices of T_m^o, the T_m^o can be obtained, while the slope

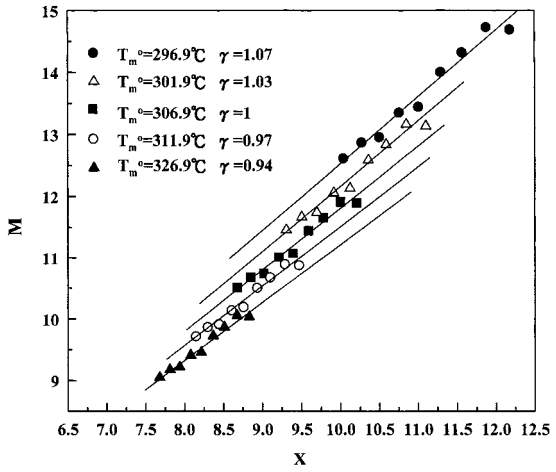

Figure 12. Plot of the scaled observed melting temperature versus the scaled crystallization temperature of sPS crystallized at different T_c from the melt (T_{max} = 345 °C) for various fittings of the equilibrium melting temperature.

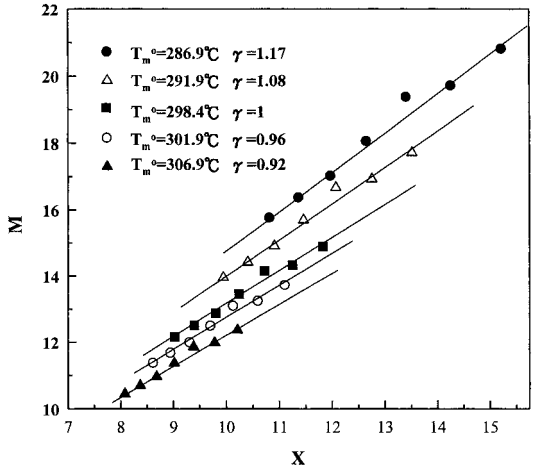

Figure 13. Plot of the scaled observed melting temperature versus the scaled crystallization temperature of sPS crystallized at different T_c from the melt (T_{max} = 290 °C) for various fittings of the equilibrium melting temperature.

of M versus X plots is equal to constant lamellar thickening coefficient, γ. This method seems to be quite simple and straightforward. However, the value of γ may depend on crystallization temperature and crystallization conditions (e.g., crystallinity). It has been suggested by Marand and co-workers that the observed melting temperature of nonthickening crystals ($\gamma = 1$ or $l = l^*$) by extrapolation of the melting temperature of thickened lamellae to zero crystallinity is much convenient to use it for the $M-X$ plots. In the sPS we studied, one interesting result was that the observed melting temperature is almost unchanged with respect to crystallinity. For comparison, the nonlinear extrapolation procedure has been applied to obtain the T_m^o in this study. We simply applied the $T_{m,0}$ previously obtained as the melting temperature of nonthickening crystals and followed the fitting procedure for the $M-X$ plots as described above. The T_m^o of β form was thus determined as an example illustrated in Figure 12. Similar data treatment has been carried out for the T_m^o of α form as shown in Figure 13. The T_m^o of β and α forms are 306.9 and 298.4 °C, respectively. The values of T_m^o obtained from the M versus X plots are indeed much higher than the results obtained from the linear Hoffman−Weeks extrapolation. Different arguments about the limitations of the various approaches for T_m^o determination have been raised to justify their validity, but that is beyond the scope of this study. We are more concerned with the effect of the polymorphism on the T_m^o. Despite the arguments, the results of structural metastability in sPS polymorphism obtained by linear extrapolation exhibits results similar to that obtained from nonlinear method.

Metastability and Transformation of Polymorphism. The equilibrium melting temperature of the β form in sPS was found to be higher than the T_m^o of the α form. On the basis of thermodynamic equilibrium, the chemical potentials of polymer repeating unit in the crystal and in the melt must be equal at equilibrium. Melting temperature is defined as the ratio of the heat of fusion, ΔH_m, to the entropy of fusion, ΔS_m (i.e., $T_m^o = \Delta H_m/\Delta S_m$). As a matter of fact, the higher value of T_m^o in the β form may be attributed to the lower value on ΔS_m and/or the higher value on ΔH_m. In other words, the Gibbs free energy, $G_c = H_c - TS_c$, of β form is lower than the α form. The orthorhombic chain packing of β form crystals is more stable than the trigonal chain packing of α form crystals. However, the experimental melting temperature of single α form is always higher than the melting temperature of single β form at the same crystallization temperature (Figure 9). This result suggests that the behaviors of sPS polymorphism exhibit a phenomenon of phase stability inversion with lamellar size as illustrated in Figure 14. This figure implies that the classical metastable state (i.e., α crystals) can become the stable one (i.e., higher melting crystals) when its phase dimensions are small enough. As it is well-known, the metastability of isothermally crystallized samples changes with lamellar size. The lower the crystallization temperature proceeds, the smaller the lamellar thickness forms and thus the lower the melting temperature appears. The melting temperature depression associated with the crystal size can be expressed quantitatively through the Gibbs−Thomson relation

$$T_m = T_m^o(1 - 2\sigma_e/l\Delta H_m)$$

where T_m is the melting point of the crystal of thickness l and σ_e is the Gibbs free surface energy of the fold-containing plane of the lamellae. While the size dependence is different for each polymorph and $(\sigma_e/\Delta H_m)_{meta} < (\sigma_e/\Delta H_m)_{stable}$, the stability of polymorphism inverts with size. Therefore, it is possible to have lower melting of β form while the morphological metastability of β form is much lower than that of α form due to the combination of reduced size and altered surface conditions. Accordingly, we speculate that the σ_e of β forms shall be much larger than the σ_e of α form.

An interesting connection between stability and kinetics may be further implied from the diagram of T_m versus $1/l$. From the viewpoint of kinetics, the smallest stable size is referred to its critical nucleus that represents the energy barrier for crystal nucleation. The smaller the critical nucleus, the faster the crystallization rate of crystalline phase. The crystallization rate of α form is, thus, expected to be faster than that of β form in the temperature range within which the crystallized lamellar thickness is less than l_Q. The induction has been further approved by the comparison of crystallization peak time, t_p, of polymorphism where the t_p of single α form is shorter than that of single β form as shown in

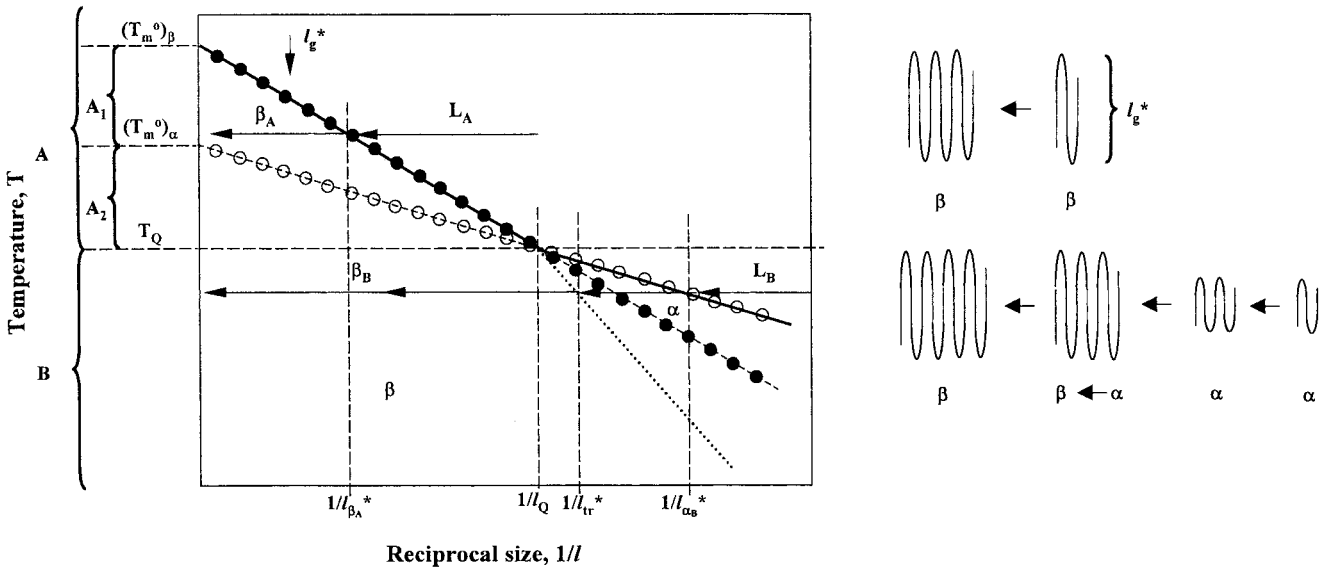

Figure 14. Temperature versus reciprocal size, 1/*l*, phase stability inversion diagram of sPS. The stable phase demarcation line is presented as a solid line (—), the metastable demarcation line is a broken line (- - -), and the phase transformation line is a dotted line (···). The pointing line (→) toward $1/l = 0$ denotes isothermal growth pathways at the crystallization temperatures, T_c. The β phase melting is presented as a filled circle line, and the α phase melting is an open circle line. The intersection of the phase lines defines a triple point Q, where all three phases (the melt L, α crystals, and β crystals) can coexist as stable phase. The growth regimes A and B are defined as the T_c above and below the triple-point temperature (T_Q), respectively. The growth pathways in regimes A and B are indicated as the pointing lines, and their corresponding molecular arrangements for chain-folding polymer crystallization are illustrated as well. The *l** refers to the sizes of limiting stability of respective phases. The thickness of $l_{\beta A}$* and $l_{\alpha B}$* are defined as the critical nucleation size of β crystals in regime A and of α crystals in regime B, respectively. The thickness of l_{tr}* indicates the limiting size for α to β phase transformation or reverse process. The growth pathway in regime A indicates the traditionally envisaged mode of growth which is exclusively lateral at fixed, kinetically determined thickness (l_g*), where $l_g^* > l_{\beta A}^*$. The growth pathway in regime B corresponds to simultaneous growth both in the lateral and the thickness directions (the thickening growth); the latter is terminated by the α to β phase transformation.[35,39]

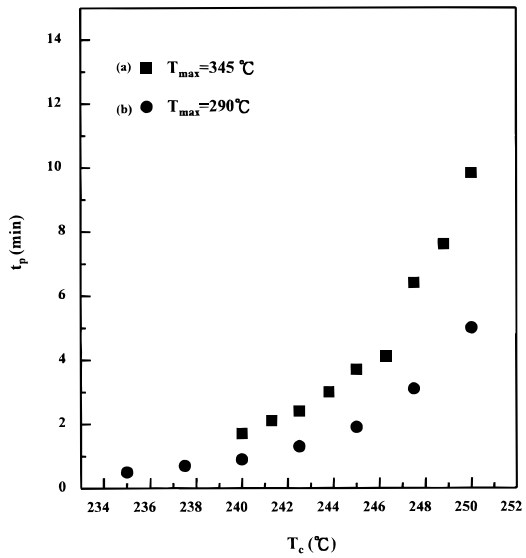

Figure 15. Crystallization peak time for sPS crystallized at different T_c from the melt (a) (T_{max} = 345 °C) and (b) (T_{max} = 290 °C).

Figure 15. Usually, the value of t_p is utilized to define the crystallization rate of isothermal crystallization. The crystallization rate is expected to be approximately proportional to the reciprocal of the peak time. The sPS is initially crystallized as α form due to the kinetic reason. The growth of α form may be either arrested or gradually transform to β form as indicated in the growth path for chain-folded polymer crystallization in region B. Surprisingly, the observation of structure transformation in sPS as illustrated in Figure 4 corresponds well to the suggested growth mechanism. The inceptive α phase gradually transforms into β phase during isothermally crystallization. Much significant experimental result with respect to the transformation was also obtained by using electron diffraction as shown in Figure 16. In the beginning of crystallization, single crystal of α″ form as identified by electron diffraction pattern of [001] zone (Figure 16a) was found. However, only the ED pattern of [001] zone having reflections of β' form (Figure 16b) was observed after long crystallization time. In the midway of crystallization period, [001] zone ED pattern of coexistence of α″ and β' phases with common molecular chain axis has been found. The detailed analysis referred to the solid−solid transformation is still under investigation and will be discussed in future report. As a result, we suggest that phase transformation from α to β phase occurs during crystallization while the limited crystal thickness is below the characteristic length of l_Q. The single α′ phase can be arrested and observed if the growing thickness is below the size of l_{tr}. Solid−solid transformation may occur on the experimental time scale as crystal growth passes the size of l_{tr}.

In addition to the transformation from α to β phase in the stage of crystal growth, clear evidence of similar transformation was found with an endothermic process during heating as illustrated in Figure 11. We propose that the transformation is attributed to the lamellar thickening process during heating. The molecular chains are able to engage rearrangement owing to chain mobility during reheating after crystallization. The tendency of thickening process can be implicitly confirmed by the formation of multiple melting. The crystal phase transforms from one state to another proceeds through different stages of metastable states according to the Ostwald stage rule. These transformations during

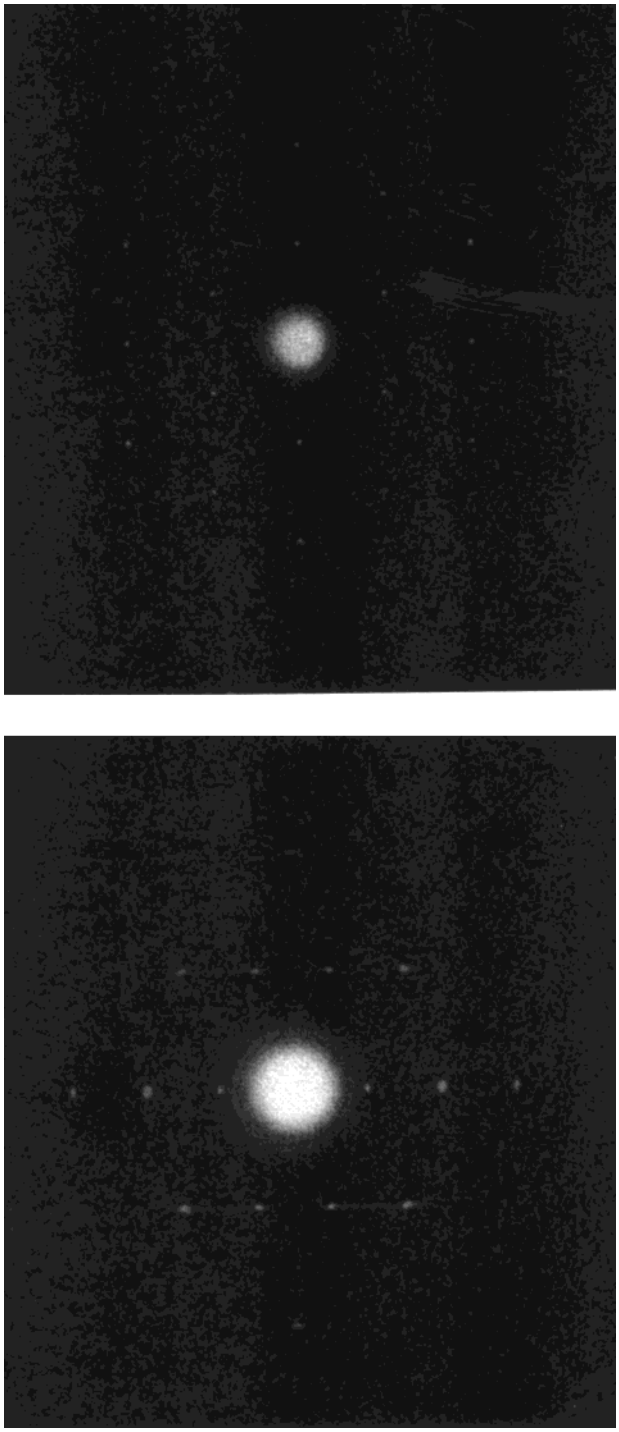

Figure 16. [001] zone electron diffraction patterns of sPS crystallized at $T_c = 245$ °C for (a) $t_c = 3$ min and (b) $t_c = 15$ min from the melt ($T_{max} = 300$ °C).

heating thus correspond to different endothermic processes. The thickening processes lead the α crystals to either form reorganized α crystals or past the l_{tr} of crystal size to achieve the structural transformation into β form. The suggested mechanism is consistent with the previous interpretations with respect to the multiple endothermic processes of melt-crystallized α crystals (Figure 11).

So far, no evidence of phase transformation from β to α phase has been found in our studies. This observation is consistent with the crystallization behavior in region A where melt-crystallized sPS directly grows as a stable β phase, and further phase transformation does not occur. However, transformation from β to α phase is, in principle, accessible if crystallization is carried out in region B and the formation of isolated β crystals are possible. As indicated in stability diagram, the initial β form may transform into α form by following the pathway of crystal growth or by simply heating crystals of specified thickness where the thickness is smaller than l_{tr}. The fact is that the expected phase transformation has not been evidenced in our studies. We speculate that such crystal thickening may be interpreted by two possible extremes based on kinetics. The thickening process of β crystals may move the experimental pathway from the initially chosen $l < l_{tr}$ toward $l = \infty$ at extremely quick process as discussed by Keller and Cheng.[34] When l becomes larger than l_{tr}, the transformed α crystals immediately enter the region of stable β crystals on further raising of temperature. Unless the WAXD recording is sufficiently rapid, the transformation from β to α form will remain unrecognized. Further experimental results by using synchrotron in-situ simultaneous WAXD and SAXS are necessary to recognize this type of transformation. The other reason may be attributed to the energy barrier to transform β crystals into α crystals that is too high to overcome. The thickening process thus passes by the pathway of structural transformation predicted by thermodynamics and enters directly to the region of stable β crystals.

Although the diagram of stability inversion is derived from thermodynamics, reasonable interpretations for the formation of polymorphism can be drawn out in terms of the kinetic concept of nucleation barrier. As found, the growth of single α phase or single β phase can be simply obtained by controlling the T_{max}. The occurrence of α phase becomes less by raising the T_{max}. This result reflects that the growth of α phase is strongly dependent upon the degree of annihilation of remaining nucleus. The size of remaining nucleus increases by reducing the T_{max} so that the energy barrier for nucleation decreases. At low enough nucleation barrier (i.e., the critical size of nucleus is smaller than l_Q), the formation rate of α crystals is faster than that of β crystals. The probability to grow α crystals thus increases owing to the fast growth rate of crystallization. The formation of α form is indeed a kinetic result of crystallization.

Conclusion

As described, polymorphism in melt-crystallized sPS is affected by a variety of factors in crystallization. In this study, the maximum annealing temperature for melt crystallization has been found to be the primary factor to determine the formed structure. Significant factors that influence the formation of polymorphism were summarized. The equilibrium melting temperatures of both forms were obtained by using linear H−W extrapolation and nonlinear H−W treatment. Both results indicate that the T_m^o of β form in sPS is higher than that of α form. In other words, the β form is more stable than the α form according to their structural metastability. In addition to structural metastability, the lamellar thickness effect (i.e., morphological metastability) has been examined. The evidences of lower melting of β phase as compared to α phase provide the fact that a structural stable phase becomes metastable if the lamellar size is small enough. Phase stability inversion with respect to the lamellar size in sPS was thus recognized. Although our understanding and ex-

perimental results for the behavior and the mechanism of phase transformation in sPS are still limited, we have found consistent interpretations of phase transformations based on phase stability inversion. We believe that the interlinkage of structural metastability and morphological metastability in sPS polymorphism shall provide the concepts and principles of transformation between metastable states and metastability in polymer phase behavior.

Acknowledgment. The financial support of the National Science Council (Grant NSC 89-2216-E-005-005) is acknowledged. The authors thank Dr. Stephen Z. D. Cheng at Institute of Polymer Science of University of Akron for his helpful discussion. R.M.H. also thanks Ms. S.-Y. Lee of Regional Instruments Center at NSYSU and Dr. S.-W. Chen of NSYSU for both their help in the WAXD experiments. We also thank Ms. P.-C. Chao of Regional Instruments Center at NCHU for her help in ED experiments.

References and Notes

(1) Guerra, G.; Vitagliano, V. M.; De Rosa, C.; Petraccone, V.; Corradini, P. *Macromolecules* **1990**, *23*, 1539.
(2) Guerra, G.; De Rosa, C.; Vitagliano, V. M.; Petraccone, V.; Corradini, P. *J. Polym. Sci., Part B: Polym. Phys.* **1991**, *29*, 265.
(3) De Rosa, C.; Guerra, G.; Petraccone, V.; Corradini, P. *Polym. J.* **1991**, *23*, 1435.
(4) De Rosa, C.; Rapacciuolo, M.; Guerra, G.; Petraccone, V.; Corradini, P. *Polymer* **1992**, *33*, 1423.
(5) Auriemma, F.; Petraccone, V.; Dal Poggetto, F.; De Rosa, C.; Guerra, G.; Manfredi, C.; Corradini, P. *Macromolecules* **1993**, *26*, 3772.
(6) Chatani, Y.; Shimance, Y.; Ijitsu, T.; Yukinari, T. *Polymer* **1993**, *34*, 1625.
(7) Manfredi, C.; Guerra, G.; De Rosa, C.; Busico, V.; Corradini, P. *Macromolecules* **1995**, *28*, 6508.
(8) De Rosa, C. *Macromolecules* **1996**, *29*, 8460.
(9) Greis, O.; Xu, Y.; Asano, T.; Petermann, J. *Polymer* **1989**, *30*, 590.
(10) Pradere, P.; Thomas, E. L. *Macromolecules* **1990**, *23*, 4954.
(11) Tosaka, M.; Hamada, N.; Tsuji, M.; Kohjiya, S.; Ogawa, T.; Isoda, S.; Kobayashi, T. *Macromolecules* **1997**, *30*, 4132.
(12) Hamada, N.; Tosaka, M.; Tsuji, M.; Kohjiya, S.; Katayama, K. *Macromolecules* **1997**, *30*, 6888.
(13) Tosaka, M.; Hamada, N.; Tsuji, M.; Kohjiya, S. *Macromolecules* **1997**, *30*, 6592.
(14) Cartier, L.; Okihara, T.; Lotz, B. *Macromolecules* **1998**, *31*, 3303.
(15) Conti, G.; Santoro, E.; Resconi, L.; Zerbi, G. *Mikrochim. Acta, Appl. Spectrosc.* **1989**, *1*, 297.
(16) Niquist, R. A. *Appl. Spectrosc.* **1989**, *43*, 440.
(17) Reynolds, N. M.; Savage, J. D.; Hsu, S. L. *Macromolecules* **1989**, *22*, 2867.
(18) Kobayashi, M.; Nakaoki, T.; Ishihara, N. *Macromolecules* **1990**, *23*, 78.
(19) Vittora, V. *Polym. Commun.* **1990**, *31*, 263.
(20) Reynolds, N. M.; Hsu, S. L. *Macromolecules* **1990**, *23*, 3463.
(21) Reynolds, N. M.; Stidham, H. D.; Hsu, S. L. *Macromolecules* **1991**, *24*, 3662.
(22) Rastogi, S.; Gupta, V. D. *J. Macromol. Sci., Phys.* **1994**, *B33*, 129.
(23) Musto, P.; Tavone, S.; Guerra, G.; De Rosa, C. *J. Polym. Sci., Part B: Polym. Phys.* **1997**, *35*, 1055.
(24) Grassi, A.; Longo, P.; Guerra, G. *Makromol. Chem. Rapid Commun.* **1989**, *10*, 687.
(25) Gomez, M. A.; Tonelli, A. E. *Macromolecules* **1990**, *23*, 3385.
(26) Capitani, D.; Segre, A. L.; Grassi, A.; Sykora, S. *Macromolecules* **1991**, *24*, 623.
(27) Capitani, D.; De Rosa, C.; Ferrando, A.; Grassi, A.; Segre, A. L. *Macromolecules* **1992**, *25*, 3874.
(28) Arnauts, J.; Berghmans, H. *Polym. Commun.* **1990**, *31*, 343.
(29) Cimmino, S.; Di Pace, E.; Martuscelli, E.; Silvestre, C. *Polymer* **1991**, *31*, 1080.
(30) Gvozdic, N. V.; Meier, D. J. *Polym. Commun.* **1991**, *32*, 493.
(31) Evans, A. M.; Kellar, E. J. C.; Knowles, J.; Galiotis, C.; Carriere, C. J.; Andrews, E. H. *Polym. Eng. Sci.* **1997**, *37*, 153.
(32) Woo, E. M.; Wu, F. S. *Macromol. Chem. Phys.* **1998**, *199*, 2041.
(33) Woo, E. M.; Sun, Y. S.; Lee, M. L. *Polymer* **1999**, *40*, 4425.
(34) Sun, Y. S.; Woo, E. M. *Macromolecules* **1999**, *32*, 7836.
(35) Keller, A.; Cheng. S. Z. D. *Polymer* **1998**, *39*, 4461.
(36) Ostwald, W. Z. *Phys. Chem.* **1897**, *22*, 286.
(37) Keller, A.; Goldbeck-Wood, G. In *Comprehensive Polymer Science*, Suppl. 2; Aggewal, A., Allen, Sir J., Ed.; Pergamon: Oxford, 1996; pp 241−305.
(38) Wunderlich, B. *Macromolecular Physics, Crystal Melting*; Academic Press: New York, 1980; Vol. III.
(39) Gutzow, I.; Toschew, S. *Krist. Tech.* **1968**, *3*, 485.
(40) Janimak, J. J.; Cheng, S. Z. D.; Zhang, A.; Hsieh, E. T. *Polymer* **1992**, *33*, 728.
(41) Hoffman, J. D.; Davis, G. T.; Lauritzen, J. I. In *Treatise on Solid State Chemistry*; Hannay, N. B., Ed.; Plenum Press: New York, 1976; Vol. III, Chapter 7.
(42) Hoffman, J. D.; Weeks, J. J. *J. Res. Natl. Bur. Stand. (U.S.)* **1962**, *A66*, 13.
(43) Huang, J.; Marand, H. *Macromolecules* **1997**, *30*, 1096.
(44) Illers, K. H. *Eur. Polym. J.* **1974**, *10*, 911.
(45) Rim, P. B.; Runt, J. P. *Macromolecules* **1984**, *17*, 1520.
(46) Marand, H.; Xu, J.; Srinivas, S. *Macromolecules* **1998**, *31*, 8219.
(47) Marand, H.; Xu, J.; Srinivas, S. *Macromolecules* **1998**, *31*, 8230.

MA000666D